DC and RF Performance of AlGaN/GaN/SiC MOSHEMTs With Deep Sub-Micron T-Gates and Atomic Layer Epitaxy MgCaO as Gate Dielectric

Hong Zhou, Xiabing Lou, Karynn Sutherlin, Jarren Summers, Sang Bok Kim, Kelson D. Chabak, Roy G. Gordon, and Peide D. Ye, *Fellow, IEEE*

***Abstract*— In this letter, we report on the dc and RF performance of AlGaN/GaN metal-oxide-semiconductor high-electron mobility transistors (MOSHEMTs) with various gate lengths (L_G) from 90 to 500 nm using atomic-layer-epitaxy single crystalline $Mg_{0.25}Ca_{0.75}O$ as gate dielectric. The 90-nm T-gate MOSHEMT simultaneously demonstrates a f_t/f_{max} of 113/160 GHz with high on/off ratio of 5×10^8. The on/off ratio increases to 2×10^{11} at $L_G = 350$ nm by reducing short channel effects. The gate leakage current is around 10^{-11} A/mm at off-state and 10^{-5} A/mm at on-state. A 160 nm L_G MOSHEMT also exhibits an output power density of 4.18 W/mm at $f = 35$ GHz and $V_{DS} = 20$ V. MgCaO demonstrates to be a promising dielectric for GaN MOS technology in serving as the surface passivation layer and reducing the gate leakage current while maintaining high RF performances for high-power applications.**

***Index Terms*— AlGaN/GaN, MOSHEMT, ALE, epitaxial oxide.**

I. Introduction

During the past two decades, GaN-based high-electron-mobility-transistors (HEMTs) have drawn intensive attention due to its wide bandgap and high saturation velocity properties, which makes it perform well for high frequency and high power applications [1]–[16]. However, there are still some issues such as high densities of surface states and high gate leakage currents which limit the performance of the devices. Surface passivation is a good approach to make the 2-dimensional electron gas (2DEG) channel immune from the surface states, originating from the dangling bonds, threading dislocations and absorbed ions from the ambient environment [17]. Gate leakage issue can be resolved by inserting a thin and wider bandgap gate dielectric in between the gate and barrier to form a higher and wider barrier to reduce the tunneling current from the gate. Considering surface passivation and minimizing gate leakage current, GaN metal-oxide-semiconductor HEMTs (MOSHEMTs) with an ultra-thin gate dielectric is an effective way to suppress gate leakage and passivate the surface in the gate-source and gate-drain regions [18].

Although GaN MOSHEMTs with amorphous gate dielectrics can partially solve the problems, real high quality oxide/barrier interfaces are still lacking. In our previous report, we have studied an epitaxial oxide (MgCaO) in a near lattice matched InAlN-GaN MOSHEMT system, and we have achieved a good DC performance [19]. However, whether this novel oxide can be applied to the conventional AlGaN/GaN system, especially for RF performance, still remains to be answered. In addition, long-term stability and reliability are also needed to verify the potential of MgCaO as a promising gate dielectric. In this letter, we successfully demonstrated the integration of the epitaxial gate dielectric MgCaO with AlGaN/GaN MOSHEMTs, showing reduced gate leakage current, high drain current (I_D) on/off ratio, negligible current collapse and hysteresis, and high RF performance.

II. Device Fabrication and Measurement

The AlGaN/GaN MOSHEMT structure was grown on a SiC substrate, consisting of, a 2-nm Al_2O_3 capping layer, a 4-nm $Mg_{0.25}Ca_{0.75}O$ epitaxial oxide, a 3-nm GaN capping layer, a 16-nm $Al_{0.26}Ga_{0.74}N$ barrier, a 1-nm AlN spacer, a GaN channel, and a 1.8-μm Fe-doped GaN buffer. Fig. 1(a) shows a cross-sectional schematic view of a T-gate AlGaN/GaN MOSHEMT on a SiC substrate. Device fabrication started with mesa isolation by Cl_2/BCl_3 etching to a depth of 80 nm. Then, Ohmic contacts were formed by depositing Ti/Al/Ni/Au

Manuscript received August 2, 2017; revised August 22, 2017; accepted August 23, 2017. Date of publication August 29, 2017; date of current version September 25, 2017. This work was supported in part by Purdue University through AFOSR monitored by Dr. K. Goretta under Grant FA9550-12-1-0180, in part by the ONR NEPTUNE Program under Grant N000141512833, and in part by Harvard University through the Center for the Next Generation of Materials by Design, an Energy Frontier Research Center from the U.S. DOE, Office of Science. The review of this letter was arranged by Editor T. Egawa. *(Corresponding author: Peide D. Ye.)*

H. Zhou and P. D. Ye are with the School of Electrical and Computer Engineering and Birck Nanotechnology Center, Purdue University, West Lafayette, IN 47907 USA (e-mail: yep@purdue.edu).

X. Lou, S. B. Kim, and R. G. Gordon are with the Department of Chemistry and Chemical Biology, Harvard University, Cambridge, MA 02138 USA.

K. Sutherlin, J. Summers, and K. D. Chabak are with the Air Force Research Laboratory, Sensors Directorate, Wright-Patterson Air Force Base, Dayton, OH 45433 USA.

Color versions of one or more of the figures in this letter are available online at http://ieeexplore.ieee.org.

Digital Object Identifier 10.1109/LED.2017.2746338

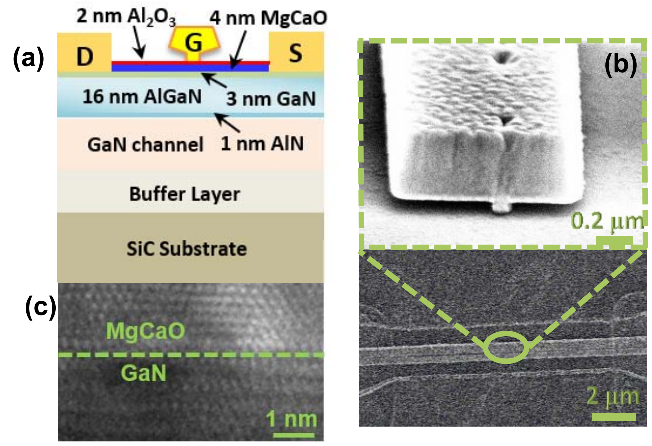

Fig. 1. (a) Schematic of a GaN MOSHEMT, (b) SEM image of the fabricated T-gate GaN MOSHEMT with L_G = 120 nm [22], and (c) TEM image of epitaxy MgCaO on GaN.

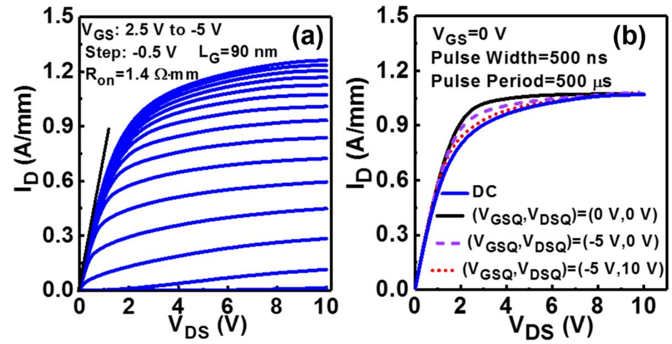

Fig. 2. (a) Output characteristics of a GaN MOSHEMT with L_G = 90 nm and L_{SD} = 2.2 μm. (b) Pulsed $I_D - V_{DS}$ measurements of the same device with 500 ns pulse width and 0.1% duty cycle.

(20/120/40/50 nm) followed by 775 °C rapid thermal anneal in N_2 atmosphere. The sheet resistance (R_{SH}) and contact resistance (R_C) were determined to be 330 $\Omega/\square$ and 0.32 Ω ·mm through transfer length method (TLM). Prior to the oxide deposition, the native oxide was etched by diluted BOE (BOE:H_2O = 1:5) for 30 s followed by soaking sample in the NH_4OH solution for 10 min for surface cleaning. 4 nm of epitaxial $Mg_{0.25}Ca_{0.75}O$ capped with 2 nm of amorphous Al_2O_3 were deposited by atomic layer epitaxy (ALE) and atomic layer deposition (ALD) chambers, respectively. The Al_2O_3 is used as capping layer to avoid MgCaO absorbing water in the following processes. More details about the oxide epitaxial growth can be found in our previous works [20]. The relative dielectric constant of MgCaO is 10. There is only 1.5% lattice mismatch between the MgCaO and the GaN capping layer, determined by X-ray diffraction (XRD) experiment, and the transmission electron microscopy (TEM) image of epitaxy MgCaO on GaN was shown in Fig. 1(c). The T-gate fabrication was carried out using a double e-beam exposures of ZEP and PMMA A10 photoresist and a dry etching Ge process [21]. The lithography processes were performed by a Vistec VB6 e-beam lithography system and a MJB3 Kurss Mask Aligner.

The devices have various T-gate foot lengths (L_G) of 90-500 nm, a source to drain spacing (L_{SD}) of 2.2 μm and a gate width of 10 and 20 μm for DC and small signal RF measurements, respectively. The T-gate head has a length of 900 nm. Fig. 1(b) shows the scanning electron microscope (SEM) image of a fabricated T-gate device with L_G of 120 nm, the same as our previous report [22], where part of device performance with L_G ≥120 nm was reported. The DC and pulse measurements were carried out with Keithley 4200 Semiconductor Characterization System and Keysight B1530A at room temperature. The RF measurements were performed using an automated system consisting of an HP4142 parametric analyzer and HP8510 network analyzer with Cascade probes.

III. Results and Discussion

Fig. 2(a) shows the well-behaved DC output characteristics (I_D-V_{DS}) of a GaN MOSHEMT with L_G = 90 nm and L_{SD} = 2.2 μm. The V_{DS} is swept from 0 V to 10 V and the V_{GS} is stepped from 2.5 V to −5 V with −0.5 V as the step. A maximum drain current density (I_{DMAX}) of 1.25 A/mm is realized at V_{DS} = 10 V and V_{GS} = 2.5 V. An on-resistance (R_{ON}) of 1.4 Ω·mm is extracted due to low R_{SH} and R_C. Fig. 2(b) depicts the current-collapse characteristics by using the 500-ns pulse width and 500-μs pulse period at room temperature. The V_{GS} is limited to be 0 V due to the current limitation (10 mA) of the pulse measurement equipment. The quiescent bias points are set at (V_{GSQ}, V_{DSQ}) = (0, 0), (−5, 0) and (−5, 10) for cold-channel, gate and drain pulses, respectively. When compared with (V_{GSQ}, V_{DSQ}) = (0, 0), the gate lag (−5, 0) seems to be negligible, showing a good passivation effect on the surface traps by the epitaxial oxide. Although there is a slight difference of 4 % current reduction between the drain lag (−5, 10) and (0, 0) near knee voltage, the drain lag I_D recovers to the same value at V_{DS} = 10 V. All the pulsed saturation currents are slightly higher than DC current, mostly likely due to a minor self-heating effect at DC.

The linear and log-scale transfer characteristics of GaN MOSHEMT are plotted in Fig. 3. A threshold voltage (V_T) of −4 V is extracted from the linear extrapolation of $I_D - V_{GS}$ at V_{DS} = 1 V for the device with L_G = 90 nm. The extrinsic peak transconductance is calculated to be 345 mS/mm at V_{DS} = 9 V and I_D = 250 mA/mm. The log-scale transfer characteristics of $I_D - V_{GS}$ clearly show a high on/off ratio of 5×10^8 at V_{DS} = 1 V. The substhreshold slope (SS) and drain induced barrier lowering (DIBL) are extracted to be 104 mV/dec (at V_{DS} = 1 V) and 110 mV/V, respectively. This SS is higher than our previous SS of InAlN/GaN MOSHEMT because of the thicker AlGaN barrier compared with the InAlN barrier [19]. We also investigate the $I_D - V_{GS}$ transfer characteristics of the AlGaN/GaN MOSHEMT with L_G = 350 nm. With a longer L_G, this device has an ultra-high on/of ratio of 2×10^{11}. The SS and DIBL are extracted to be 63 mV/dec and 35 mV/V due to the minimized short channel effects (SCE). Fig. 3(b) reveals a low hysteresis of 30 mV when V_{GS} is swept from −7 V to 3V and then swept back. It indicates high quality of MgCaO/GaN interface. In addition, the gate leakage current is reduced by several orders of magnitude compared with HEMT [23] on both the

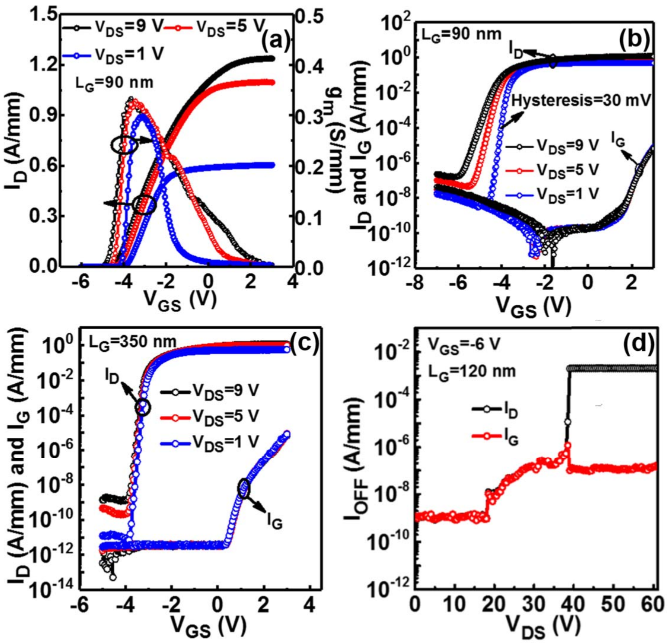

Fig. 3. (a) Linear plot of $g_m - V_{GS}$ and $I_D - V_{GS}$ transfer characteristics of the device with $L_G = 90$ nm and $L_{SD} = 2.2$ μm. (b) Log-scale plot of the $I_D - I_G - V_{GS}$ with a dual sweep of the V_{GS}. (c) Log-scale plot of the $I_D - I_G - V_{GS}$ of another device with $L_G = 350$ nm. Ultra-high on/off ratio of 2×10^{11} and low SS = 63 mV/dec are obtained. (d) Three-terminal off-state breakdown measurement of the device with $L_G = 120$ nm and $L_{SD} = 2.2$ μm.

on-state and off-state, which can potentially help to improve device reliability. Finally, benefiting from the ultra-low leakage of the AlGaN/GaN MOSHEMT, device with $L_G = 120$ nm and $L_{SD} = 2.2$ μm demonstrates a high three-terminal off-state breakdown voltage (BV_{GD}) of 39 V as shown in Fig. 3(d).

Fig. 4(a) depicts the small-signal RF measurements of one representative device with $L_G = 90$ nm biased at the peak g_m condition and $V_{DS} = 9$ V. The off-wafer standard LRRM calibration is used to calibrate the network analyzer and the on-wafer open and short structures are used to de-embed the pad parasitic from the as-measured S-parameter. The unity current gain cut-off frequency (f_t) is given by linear extrapolation of the linear region of the H_{21} gain at low f regions. The maximum oscillation frequency (f_{max}) is determined by the extrapolation of the linear region of the gain at low frequency extrapolation of the maximum available gain (MAG) through a conservative −20 dB/dec slope methodology. The gate to source capacitance (C_{gs}) and gate to drain capacitance (C_{gd}) of this $L_G = 90$ nm device are extracted to be 0.29 and 0.09 pF/mm, respectively. A f_t/f_{max} of 113/160 GHz and 101/150 GHz are extracted for $L_G = 90$ nm and 120 nm devices, yielding a high $f_t \cdot L_G$ of 10.2 GHz·μm and 12 GHz·μm with L_G to total barrier-thickness (d) ratio of 3.46 and 4.6, respectively. Combining with the $BV_{GD} = 39$ V, device with $L_G = 120$ nm possesses a Johnson's-Figure-of-Merit (J-FOM, $BV_{GD} \times f_t$) of 4 THz·V. This value is comparable to the state-of-art J-FOM of AlGaN/GaN HEMT and MOSHEMTs [24]–[26]. Fig. 4(b) shows the L_G dependent f_t and f_{max} scaling behaviors of GaN MOSHEMT. The peak

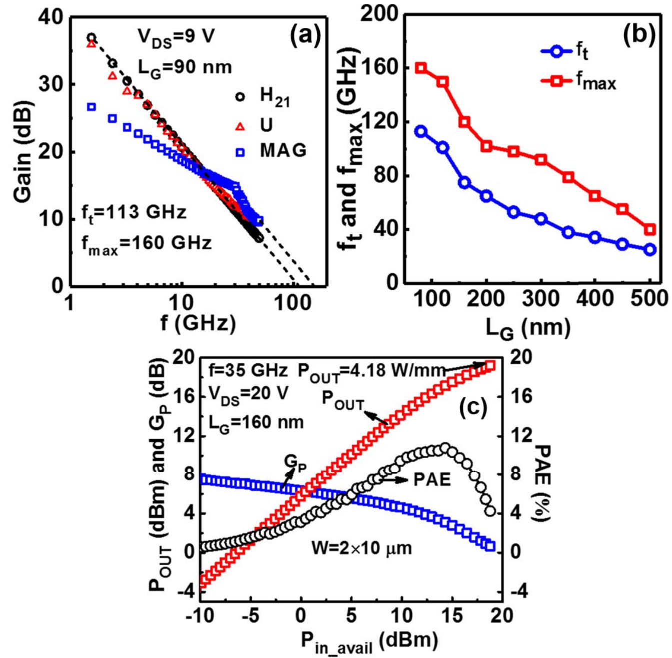

Fig. 4. (a) Pad deembedded small-signal RF performance of a GaN MOSHEMT with $L_G = 90$ nm (b) f_T and f_{max} scaling metrics of the GaN MOSHEMTs (c) Large-signal deep class-AB performance of a $L_G = 160$ nm device with power-sweep at f = 35 GHz and $V_{DS} = 20$ V.

$f_t \cdot L_G$ value of 14.2 GHz·μm is achieved at $L_G = 300$ nm. Representative deep class-AB load-pull curves at f = 35 GHz with input and output matched for high-power are shown in Fig. 4(c). The measured source and load impedance for load-pull measurement is 47.48+j×92.34Ω and 158.8+j×160.1Ω, respectively. A decent output power density (P_{OUT}) of 4.18 W/mm is achieved at $V_{DS} = 20$ V. As a reference, Crespo et al. in AFRL have demonstrated a 9.8 nm barrier InAlN/GaN HEMT with $P_{OUT} = 5.8$ W/mm at a $L_G = 160$ nm and $L_{SD} = 2.8$ μm [27]. Considering the lower I_D and L_G/d of 4.6 of AlGaN MOSHEMT compared with InAlN HEMT with L_G/d = 16, our result shows potential scaling and improvement when the barrier can be further scaled.

IV. Conclusion

ALE MgCaO has been shown to be a good passivation layer and gate insulator in T-gate AlGaN/GaN MOSHEMTs. High on/off ratio, negligible current collapse and hysteresis result from the nearly lattice-matched MgCaO/GaN epitaxial interface. A combination of f_t and f_{max} of 113 GHz and 160 GHz have been achieved for a $L_G = 90$ nm GaN MOSHEMT with on/off ratio of 5×10^8. A P_{OUT} of 4.18 W/mm has also been demonstrated at f = 35 GHz. ALE MgCaO offers the promise of AlGaN/GaN MOSHEMTs with increased performance in microwave and millimeter-wave high-power applications.

References

[1] Y. Tang, K. Shinohara, D. Regan, A. Corrion, D. Brown, J. Wong, A. Schmitz, H. Fung, S. Kim, and M. Micovic, "Ultrahigh-speed GaN high-electron-mobility transistors with f_T/f_{max} of 454/444 GHz," *IEEE Electron Device Lett.*, vol. 36, no. 6, pp. 549–551, Jun. 2015, doi: 10.1109/LED.2015.2421311.

[2] Y. Yue, Z. Hu, J. Guo, B. Sensale-Rodriguez, G. Li, R. Wang, F. Faria, T. Fang, B. Song, X. Gao, S. Guo, T. Kosel, G. Snider, P. Fay, D. Jena, and H. Xing, "InAlN/AlN/GaN HEMTs with regrown ohmic contacts and f_T of 370 GHz," *IEEE Electron Device Lett.*, vol. 33, no. 7, pp. 988–990, Jul. 2012, doi: 10.1109/LED.2012.2196751.

[3] D. S. Lee, X. Gao, S. Guo, D. Kopp, P. Fay, and T. Palacios, "300-GHz InAlN/GaN HEMTs with InGaN back barrier," *IEEE Electron Device Lett.*, vol. 32, no. 11, pp. 1525–1527, Nov. 2011, doi: 10.1109/LED.2011.2164613.

[4] Y.-F. Wu, A. Saxler, M. Moore, R. P. Smith, S. Sheppard, P. M. Chavarkar, T. Wisleder, U. K. Mishra, and P. Parikh, "30-W/mm GaN HEMTs by field plate optimization," *IEEE Electron. Device Lett.*, vol. 25, no. 3, pp. 117–119, Mar. 2004, doi: 10.1109/LED.2003.822667.

[5] K. Shinohara, D. Regan, A. Corrion, D. Brown, S. Burnham, P. J. Willadsen, I. Alvarado-Rodriguez, M. Cunningham, C. Butler, A. Schmitz, S. Kim, B. Holden, D. Chang, V. Lee, A. Ohoka, P. M. Asbeck, and M. Micovic, "Deeply-scaled self-aligned-gate GaN DH-HEMTs with ultrahigh cutoff frequency," in *IEDM Tech. Dig.*, Dec. 2011, pp. 19.1.1–19.1.4, doi: 10.1109/IEDM.2011.6131582.

[6] D. Xu, K. K. Chu, J. A. Diaz, M. Ashman, J. J. Komiak, L. M. Pleasant, C. Creamer, K. Nichols, K. H. G. Duh, P. M. Smith, P. C. Chao, L. Dong, and P. D. Ye, "0.1-μm atomic layer deposition Al_2O_3 passivated InAlN/GaN high electron-mobility transistors for E-band power amplifiers," *IEEE Electron Device Lett.*, vol. 36, no. 5, pp. 442–444, May 2015, doi: 10.1109/LED.2015.2409264.

[7] H. Sun, A. R. Alt, H. Benedickter, E. Feltin, J.-F. Carlin, M. Gonschorek, N. Grandjean, and C. R. Bolognesi, "205-GHz (Al,In)N/GaN HEMTs," *IEEE Electron Device Lett.*, vol. 31, no. 9, pp. 957–959, Sep. 2010, doi: 10.1109/LED.2010.2055826.

[8] X. Zheng, M. Guidry, E. Ahmadi, K. Hestroffer, B. Romanczyk, S. Wienecke, S. Keller, and U. K. Mishra, "N-polar GaN MIS-HEMTs on sapphire with high combination of power gain cutoff frequency and three-terminal breakdown voltage," *IEEE Electron Device Lett.*, vol. 37, no. 1, pp. 77–80, Jan. 2016, doi: 10.1109/LED.2015.2502253.

[9] K. D. Chabak, M. Trejo, A. Crespo, D. E. Walker, J. Yang, R. Gaska, M. Kossler, J. K. Gillespie, G. H. Jessen, V. Trimble, and G. D. Via, "Strained AlInN/GaN HEMTs on SiC with 2.1-A/mm output current and 104-GHz cutoff frequency," *IEEE Electron Device Lett.*, vol. 31, no. 6, pp. 561–563, Jun. 2010, doi: 10.1109/LED.2010.2045099.

[10] K. D. Chabak, D. E. Walker, M. R. Johnson, A. Crespo, A. M. Dabiran, D. J. Smith, A. M. Wowchak, S. K. Tetlak, M. Kossler, J. K. Gillespie, R. C. Fitch, and M. Trejo, "High-performance AlN/GaN HEMTs on sapphire substrate with an oxidized gate insulator," *IEEE Electron Device Lett.*, vol. 32, no. 12, pp. 1677–1679, Dec. 2011, doi: 10.1109/LED.2011.2167952.

[11] D. S. Lee, O. Laboutin, Y. Cao, W. Johnson, E. Beam, A. Ketterson, M. Schuette, P. Saunier, and T. Palacios, "Impact of Al_2O_3 passivation thickness in highly scaled GaN HEMTs," *IEEE Electron Device Lett.*, vol. 33, no. 7, pp. 976–978, Jul. 2012, doi: 10.1109/LED.2012.2194691.

[12] B. Song, B. Sensale-Rodriguez, R. Wang, A. Ketterson, M. Schuette, E. Beam, P. Saunier, X. Gao, S. Guo, P. Fay, D. Jena, and H. G. Xing, "Monolithically integrated E/D-mode InAlN HEMTs with $f_t/f_{\max} >$ 200/220 GHz," in *Proc. 70th Annu. DRC*, Jun. 2012, pp. 1–2, doi: 10.1109/DRC.2012.6257009.

[13] M. Higashiwaki, T. Mimura, and T. Matsui, "AlGaN/GaN heterostructure field-effect transistors on 4H-SiC substrates with current-gain cutoff frequency of 190 GHz," *Appl. Phys. Exp.*, vol. 1, no. 2, p. 021103, Feb. 2008, doi: 10.1143/APEX.1.021103.

[14] A. L. Corrion, K. Shinohara, D. Regan, I. Milosavljevic, P. Hashimoto, P. J. Willadsen, A. Schmitz, S. J. Kim, C. M. Butler, D. Brown, S. D. Burnham, and M. Micovic, "High-speed AlN/GaN MOS-HFETs with scaled ALD Al_2O_3 gate insulators," *IEEE Electron Device Lett.*, vol. 32, no. 8, pp. 1062–1064, Aug. 2011, doi: 10.1109/LED.2011.2155616.

[15] D. J. Meyer, D. A. Deen, D. F. Storm, M. G. Ancona, D. S. Katzer, R. Bass, J. A. Roussos, B. P. Downey, S. C. Binari, T. Gougousi, T. Paskova, E. A. Preble, and K. R. Evans, "High electron velocity submicrometer AlN/GaN MOS-HEMTs on freestanding GaN substrates," *IEEE Electron Device Lett.*, vol. 34, no. 2, pp. 199–201, Feb. 2013, doi: 10.1109/LED.2012.2228463.

[16] J. S. Moon, S. Wu, D. Wong, I. Milosavljevic, A. Conway, P. Hashimoto, M. Hu, M. Antcliffe, and M. Micovic, "Gate-recessed AlGaN-GaN HEMTs for high-performance millimeter-wave applications," *IEEE Electron Device Lett.*, vol. 26, no. 6, pp. 348–350, Jun. 2005, doi: 10.1109/LED.2008.2000792.

[17] B. M. Green, K. K. Chu, E. M. Chumbes, J. A. Smart, J. R. Shealy, and L. F. Eastman, "The effect of surface passivation on the microwave characteristics of undoped AlGaN/GaN HEMTs," *IEEE Electron Device Lett.*, vol. 21, no. 6, pp. 268–270, Jun. 2000, doi: 10.1109/55.843146.

[18] P. D. Ye, B. Yang, K. K. Ng, J. Bude, G. D. Wilk, S. Halder, and J. C. M. Hwang, "GaN metal-oxide-semiconductor high-electron-mobility-transistor with atomic layer deposited Al_2O_3 as gate dielectric," *Appl. Phys. Lett.*, vol. 86, no. 6, pp. 063501-1–063501-3, Feb. 2005, doi: 10.1063/1.1861122.

[19] H. Zhou, X. B. Lou, N. J. Conrad, M. W. Si, H. Wu, S. Alghamdi, S. P. Guo, R. G. Gordon, and P. D. Ye, "High-performance InAlN/GaN MOSHEMTs enabled by atomic layer epitaxy MgCaO as gate dielectric," *IEEE Electron Device Lett.*, vol. 37, no. 5, pp. 556–559, May 2016, doi: 10.1109/LED.2016.2537198.

[20] X. Lou, H. Zhou, S. B. Kim, S. Alghamdi, X. Gong, J. Feng, X. Wang, P. D. Ye, and R. G. Gordon, "Epitaxial growth of $Mg_xCa_{1-x}O$ on GaN by atomic layer deposition," *Nano Lett.*, vol. 16, no. 12, pp. 7650–7654, Nov. 2016, doi: 10.1021/acs.nanolett.6b03638.

[21] T. Palacios, E. Snow, Y. Pei, A. Chakraborty, S. Keller, S. P. DenBaars, and U. K. Mishra, "Ge-spacer technology in AlGaN/GaN HEMTs for mm-wave applications," in *IEDM Tech. Dig.*, Dec. 2005, pp. 1–3, doi: 10.1109/IEDM.2005.1609472.

[22] H. Zhou, K. Sutherlin, X. Lou, S. B. Kim, K. D. Chabak, R. G. Gordon, and P. D. Ye, "DC and RF characterizations of AlGaN/GaN MOSHEMTs with deep sub-micron T-gates and atomic layer epitaxy MgCaO as gate dielectric," in *Proc. 74th Annu. Device Res. Conf. (DRC)*, Jun. 2016, pp. 1–2, doi: 10.1109/DRC.2016.7548407.

[23] D. Xu, K. Chu, J. Diaz, W. Zhu, R. Roy, L. M. Pleasant, K. Nichols, P.-C. Chao, M. Xu, and P. D. Ye, "0.2-μm AlGaN/GaN high electron-mobility transistors with atomic layer deposition Al_2O_3 passivation," *IEEE Electron Device Lett.*, vol. 34, no. 6, pp. 744–746, Jun. 2013, doi: 10.1109/LED.2013.2255257.

[24] S. Huang, K. Wei, G. Liu, Y. Zheng, X. Wang, L. Pang, X. Kong, X. Liu, Z. Tang, S. Yang, Q. Jiang, and K. J. Chen, "High-f_{MAX} high Johnson's figure-of-merit 0.2-μm gate AlGaN/GaN HEMTs on silicon substrate with AlN/SiN_x passivation," *IEEE Electron Device Lett.*, vol. 35, no. 3, pp. 315–317, Mar. 2014, doi: 10.1109/LED.2013.2296354.

[25] S. Arulkumaran, G. I. Ng, and S. Vicknesh, "Enhanced breakdown voltage with high Johnson's figure-of-merit in 0.3-μm T-gate AlGaN/GaN HEMTs on silicon by $(NH_4)_2S_x$ treatment," *IEEE Electron Device Lett.*, vol. 34, no. 11, pp. 1364–1366, Nov. 2013, doi: 10.1109/LED.2013.2279882.

[26] S. Yoshida, M. Tanomura, Y. Murase, K. Ota, K. Matsunaga, and H. Shimawaki, "A 76 GHz GaN-on-silicon power amplifier for automotive radar systems," in *IEEE MTT-S Int. Microw. Symp. Dig.*, Jun. 2009, pp. 665–668, doi: 10.1109/MWSYM.2009.5165784.

[27] A. Crespo, M. M. Bellot, K. D. Chabak, J. K. Gillespie, G. H. Jessen, V. Miller, M. Trejo, G. D. Via, D. E. Walker, B. W. Winningham, H. E. Smith, T. A. Cooper, X. Gao, and S. Guo, "High-power Ka-band performance of AlInN/GaN HEMT with 9.8-nm-thin barrier," *IEEE Electron Device Lett.*, vol. 31, no. 1, pp. 2–4, Jan. 2010, doi: 10.1109/LED.2009.2034875.